Topological Dependence of Runaway Avalanche Threshold in Momentum Space

Chris McDevitt

In collaboration with: Zehua Guo and Xianzhu Tang

Los Alamos National Laboratory

Work supported by SCREAM SciDAC

Outline

- Runaway Vortex: Momentum space topology of primary runaway distribution function
- Link of avalanche threshold to momentum space topological change ⇔ O-X merger (disappearance of runaway vortex)
- Self-consistent formulation of small and large angle collisions ➔ Impact on avalanche threshold and growth rate

Motivation: Avalanche Threshold

- The avalanche threshold is a crucial quantity for disruption mitigation scenarios
  - Provides guidance as to what conditions are necessary in order to avoid runaway generation through secondary generation
- An accurate prediction of the avalanche threshold has proven difficult:
  - Large amounts of high-Z materials typically present ⇔ resulting collisional coefficients highly complex (free-bound, scattering by partially shielded nucleus, etc) [Breizman IAEA 2016, Hesslow et al. 2017]
  - Runaway models typically make different modeling assumptions ⇔ leads to order one variation of avalanche threshold [Rosenbluth-Putvinski 1997–Martin-Solis 2017]
- Here we are interested in identifying a robust indicator of the avalanche threshold
  - Independent of specific model assumptions

Runaway Electrons

- Runaway electrons may be present when the parallel electric field overcomes the collisional drag
  - In the absence of other physics electrons can be accelerated to arbitrarily high energies
  - Critical electric field above which electrons are accelerated given by Connor-Hastie threshold E_c

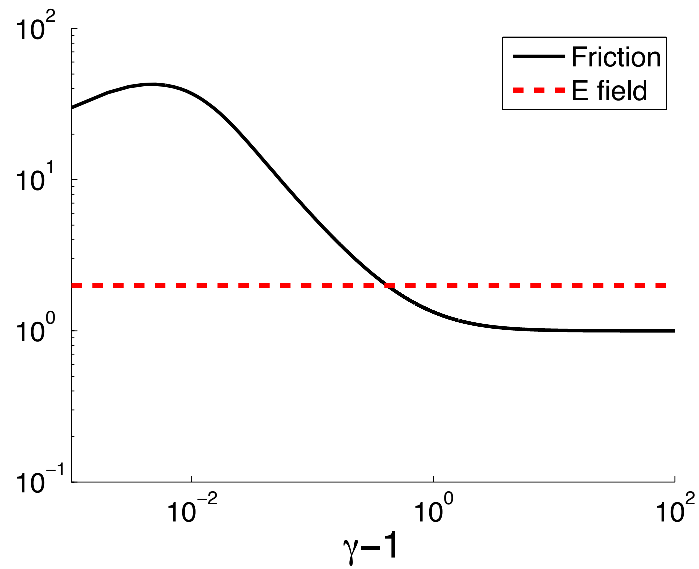

- Energy of runaway electrons thought to be limited by radiation:
  - Bremsstrahlung radiation: likely most important for dense plasmas with a large impurity content
  - Synchrotron radiation: most important mechanism in a range of parameter regimes (Guo et al. 2017)

Formation of Primary Electron Tail

- For $E > E_c$ electrons in a broad region of momentum space capable of running away

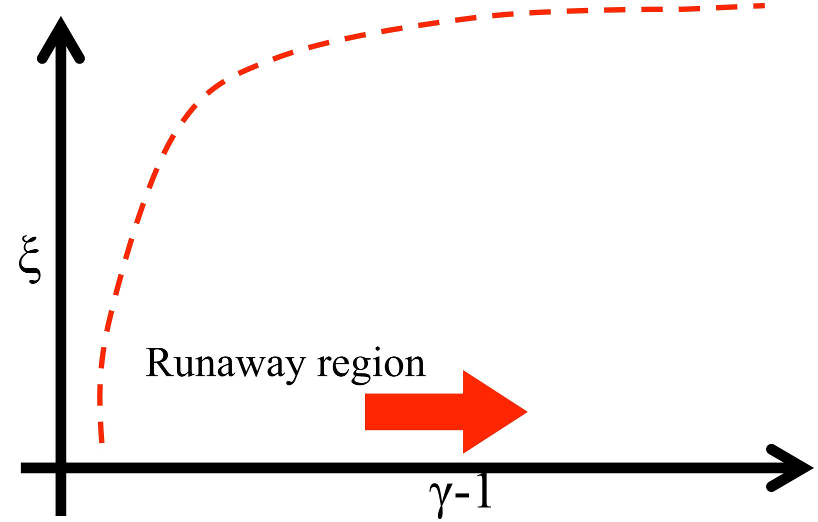

Formation of Primary Electron Tail

- For $E > E_c$ electrons in a broad region of momentum space capable of running away
  - Presence of synchrotron radiation constrains "runaway" region
  - Synchrotron radius damps perpendicular energy ⇔ narrow "channel" along ξ=-1 axis present

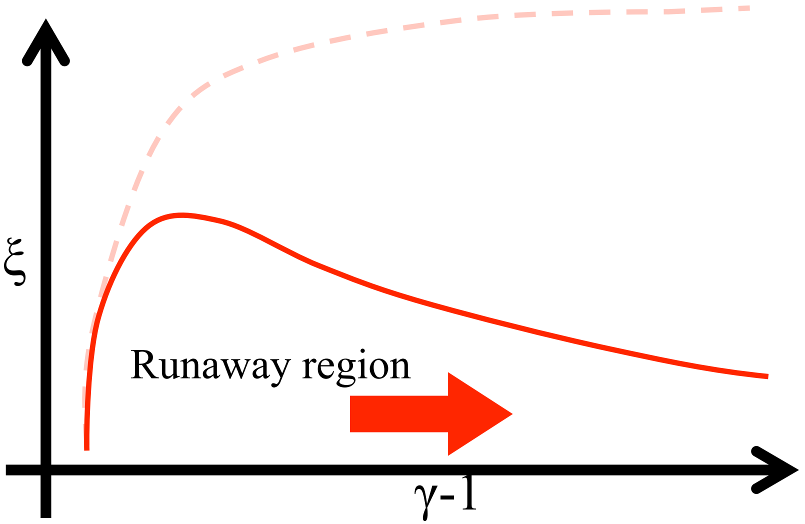

Formation of Primary Electron Tail

- For $E > E_c$ electrons in a broad region of momentum space capable of running away
  - Presence of synchrotron radiation constrains "runaway" region
  - Synchrotron radius damps perpendicular energy ⇔ narrow "channel" along ξ=-1 axis present
  - Pitch-angle scattering capable of transporting electrons out of channel ⇔ electrons slow down due to sync. rad.

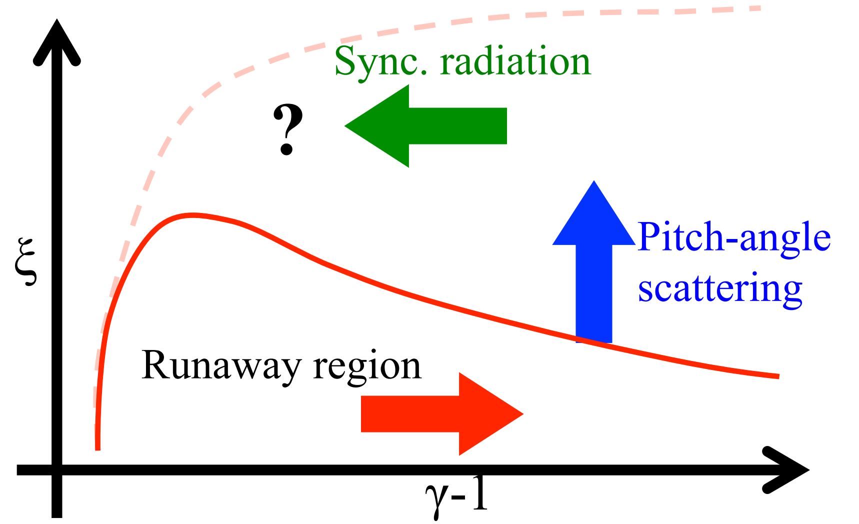

Formation of Primary Electron Tail

- For $E > E_c$ electrons in a broad region of momentum space capable of running away
  - Presence of synchrotron radiation constrains “runaway” region
  - Synchrotron radius damps perpendicular energy ⇔ narrow “channel” along ξ=-1 axis present
  - Pitch-angle scattering capable of transporting electrons out of channel ⇔ electrons slow down due to sync. rad.

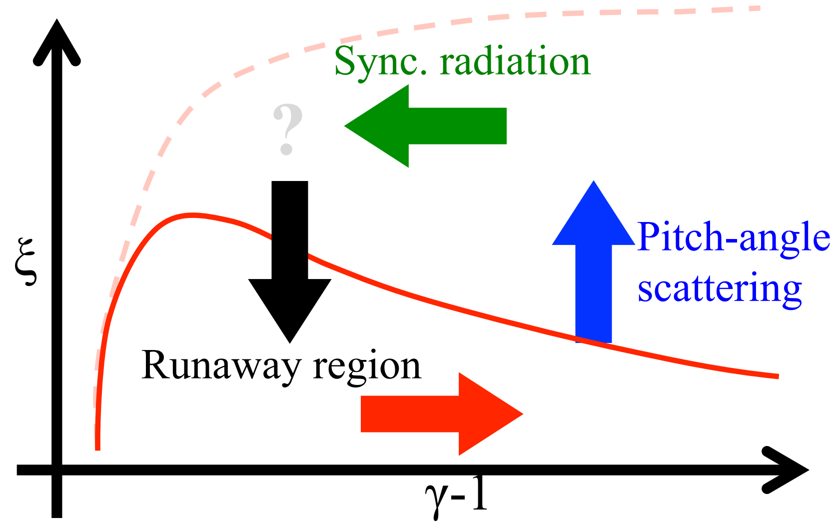

1. For a sufficiently strong electric field, primary electrons are pinched back to ξ=-1 axis ➔ runaway vortex
   - Leads to confinement of runaway electron population

Formation of Primary Electron Tail

- For $E > E_c$ electrons in a broad region of momentum space capable of running away
  - Presence of synchrotron radiation constrains "runaway" region
  - Synchrotron radius damps perpendicular energy ⇔ narrow "channel" along ξ=-1 axis present
  - Pitch-angle scattering capable of transporting electrons out of channel ⇔ electrons slow down due to sync. rad.

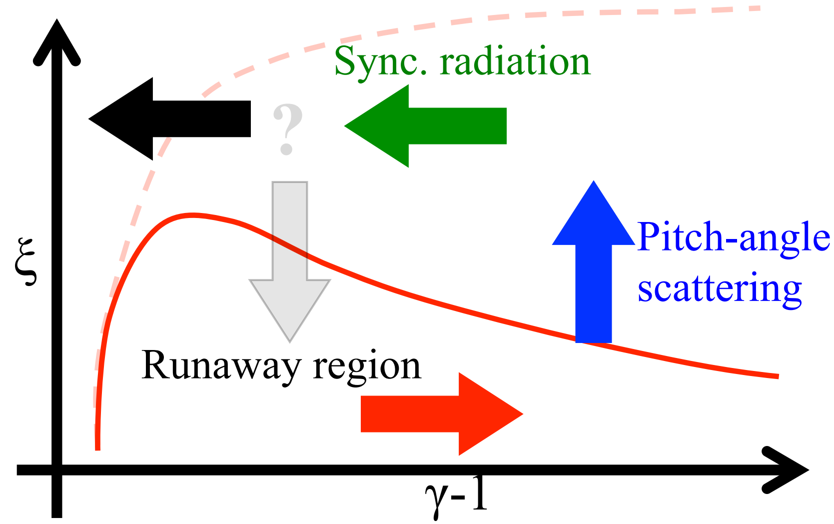

1. For a sufficiently strong electric field, primary electrons are pinched back to ξ=-1 axis ➔ runaway vortex
   - Leads to confinement of runaway electron population

2. For weaker electric fields, primary electrons return to bulk:
   - Pitch-angle scattering prevents electrons from collapsing onto ξ=-1 axis
   - No effective means of confining runaway electrons

O-X Merger of Primary Distribution

- Topology of momentum space flows distinct for the two cases discussed above (Guo et al. 2017)
- Above threshold:
  - Runaway vortex present at high energy
  - Provides a means of confining runaway electrons
- Below threshold:
  - All flux lines return to electron bulk
  - No means of confining runaway electrons
- Threshold for runaway vortex distinct from Connor-Hastie threshold:

$$\boxed{E_{ox} > E_c}$$

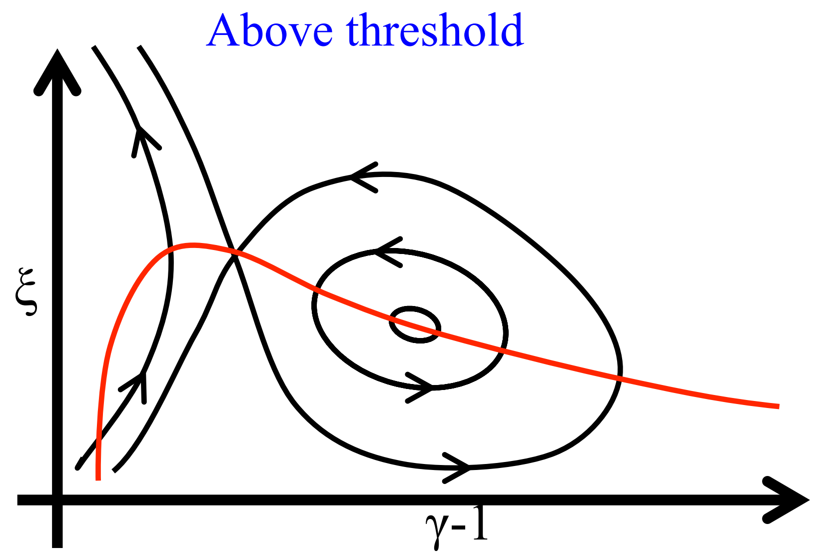

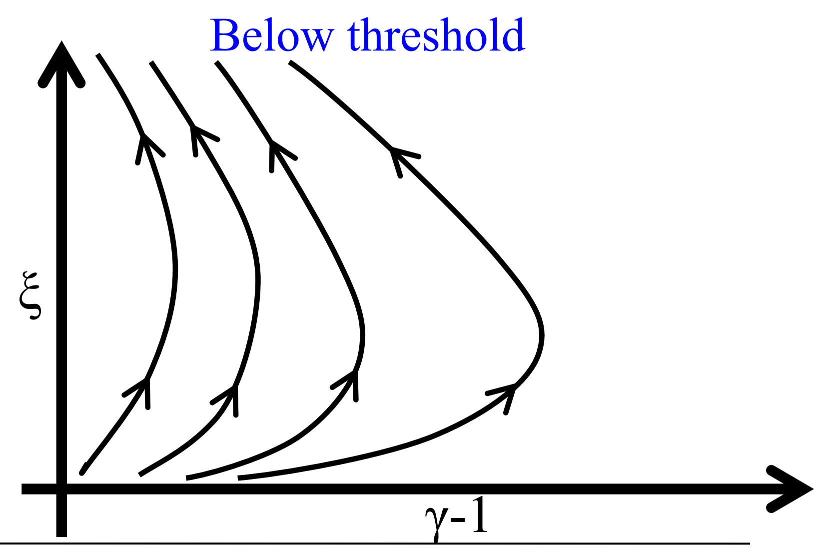

Los Alamos NATIONAL LABORATORY EST.1943

NNSA

Primary Runaway Distribution

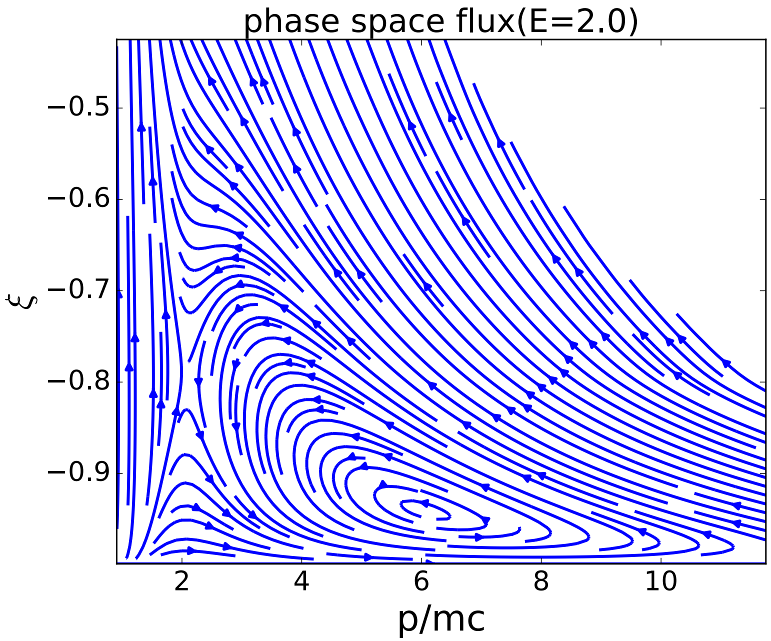

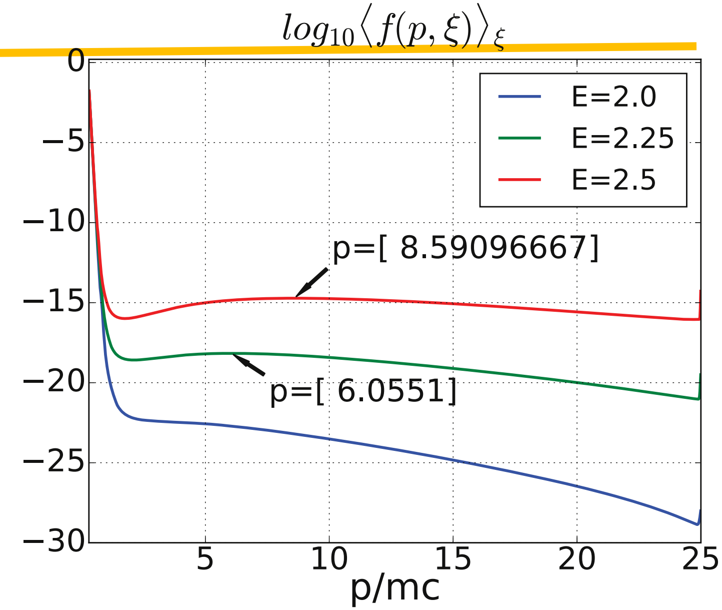

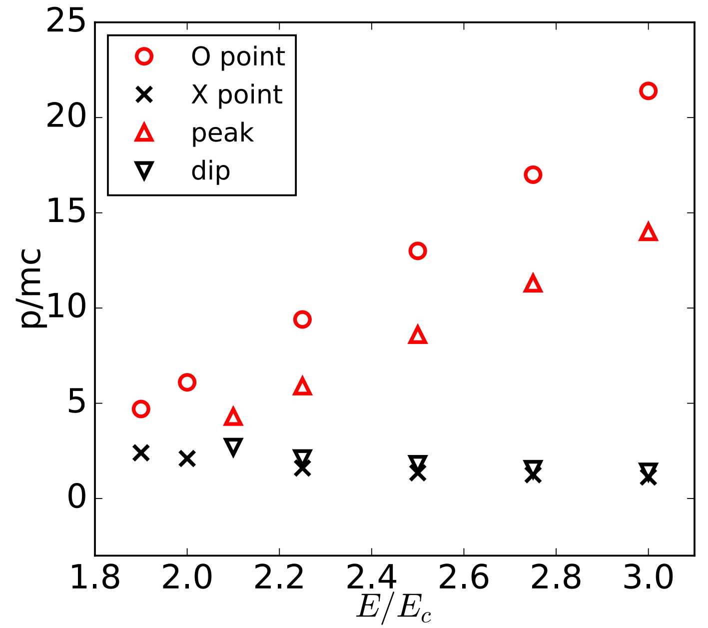

- Bump and energy spread of distribution set by runaway vortex
- Threshold for bump is distinct from O-X merger threshold $E_b > E_{ox}$
  - Presence of runaway vortex does not imply a bump in runaway distribution

Outline

- Runaway Vortex: Momentum space topology of primary runaway distribution function

- Link of avalanche threshold to momentum space topological change ⇔ O-X merger (disappearance of runaway vortex)

- Self-consistent formulation of small and large angle collisions ➔ Impact on avalanche threshold and growth rate

Source of Secondary Electrons ➔ Avalanche

- Avalanche instability arises due to large-angle collisions of runaways with thermal electrons
- Rosenbluth-Putvinski (RP) secondary source provides a particularly simple picture:
  - Runaway electrons assumed to be located at infinite energy on pitch-angle axis
  - Fraction of "secondary" electrons kicked into runaway region ⇔ leads to exponential growth of runaway population

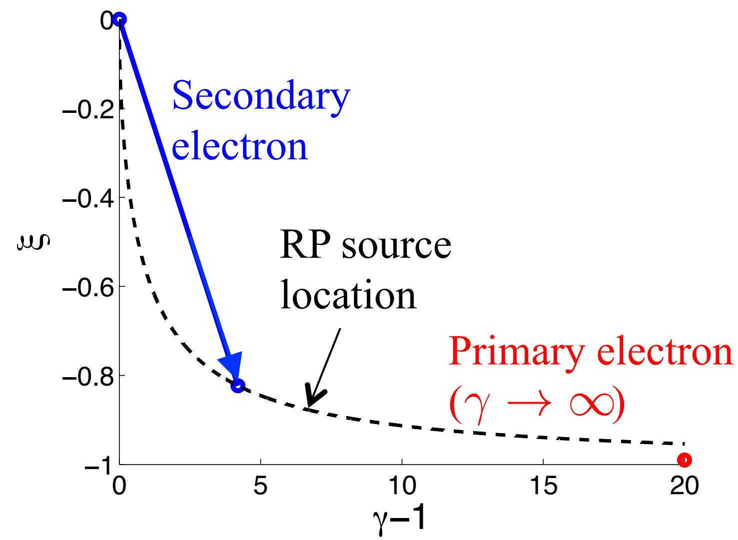

Source of Secondary Electrons ➔ Avalanche

- Avalanche instability arises due to large-angle collisions of runaways with thermal electrons
- Rosenbluth-Putvinski (RP) secondary source provides a particularly simple picture:
  - Runaway electrons assumed to be located at infinite energy on pitch-angle axis
  - Fraction of "secondary" electrons kicked into runaway region ⇔ leads to exponential growth of runaway population
- A simple extension of the above model is to account for the energy/pitch-angle distribution of the primary electrons
  - Leads to a distributed source of secondary electrons

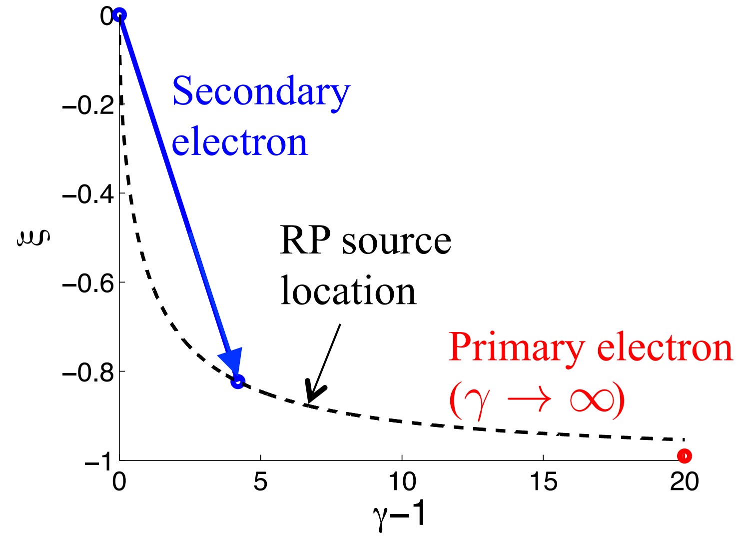

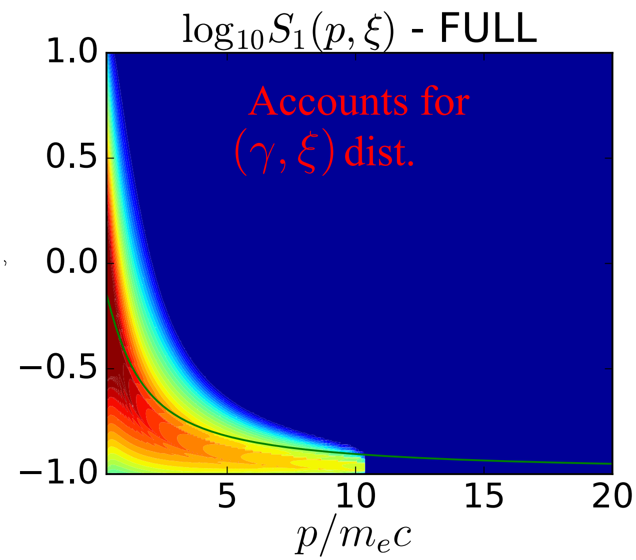

Runaway Electron Solvers

- The relativistic Fokker-Planck equation is solved via two distinct approaches:
- Particle based solver
  - Pitch-angle diffusion described by Monte Carlo collision operator [Boozer 1981], energy diffusion neglected
  - Absorbing boundary condition assumed at low energy

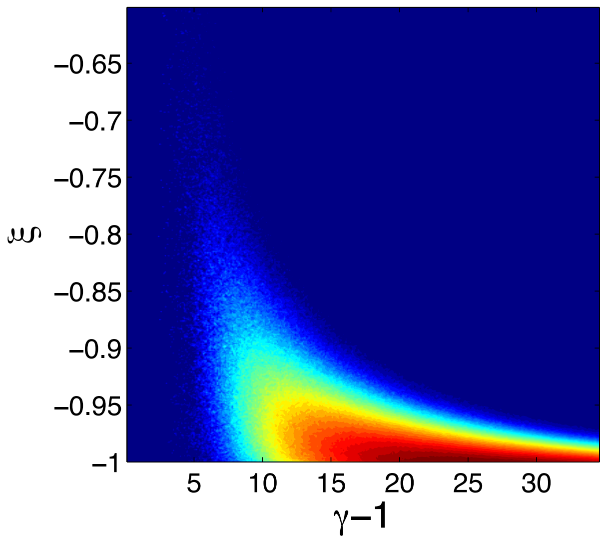

- Continuum Fokker-Planck solver [Guo 2017]
  - Considers direct solution of Fokker-Planck equation
  - Solves for tail electron distribution while matching to a Maxwellian-Jüttner distribution at low energy
  - Allows for accurate calculation of momentum space fluxes ⇔ momentum space topology

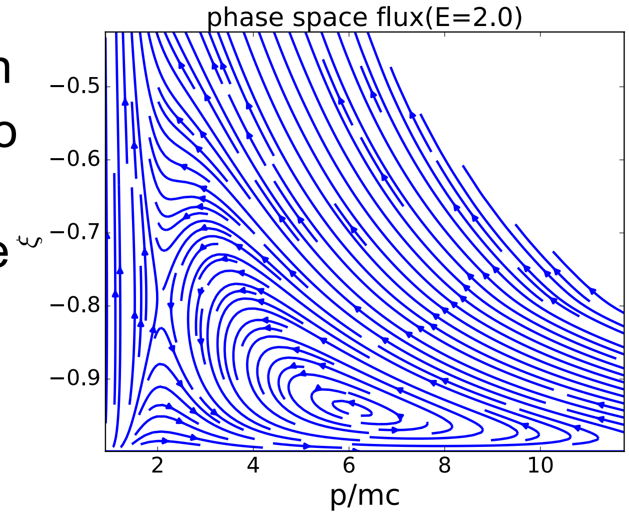

Los Alamos
NATIONAL LABORATORY
EST. 1943

NNSA

A Common Model of Avalanche Instability

- Model includes [Liu et al. 2017]:
  - Distributed secondary source term
  - Test-particle collision operator
  - Synchrotron radiation used to limit the runaway's energy

$$\frac{\partial f_e}{\partial t} - \bar{E}\left(\xi \frac{\partial f_e}{\partial p}\right) + \frac{1-\xi^2}{p}\frac{\partial f_e}{\partial \xi} = C\left(f_e\right) + C_{rad}\left(f_e\right) + S_{sec}\left(f_e\right)$$

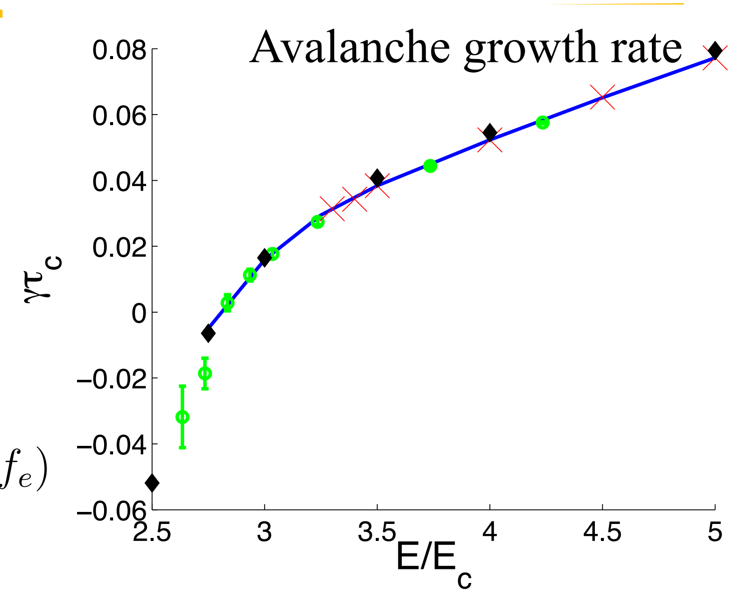

- Model involves several idealizations:
  - Does not incorporate self-consistent down-scattering of primary electrons
  - Uses constant Coulomb logarithm

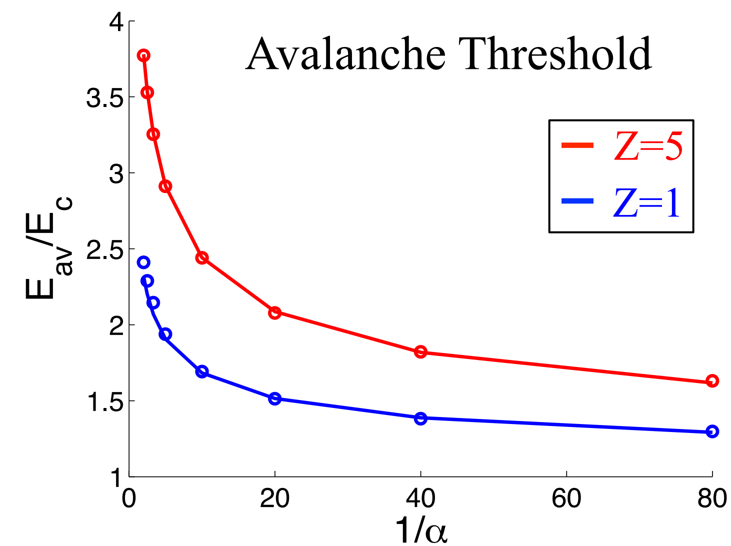

Avalanche growth rate and threshold accurately reproduced by both the particle and continuum Fokker-Planck solvers

Los Alamos NATIONAL LABORATORY EST. 1943

NNSA

Relation of Avalanche Threshold to Features of Primary Distribution

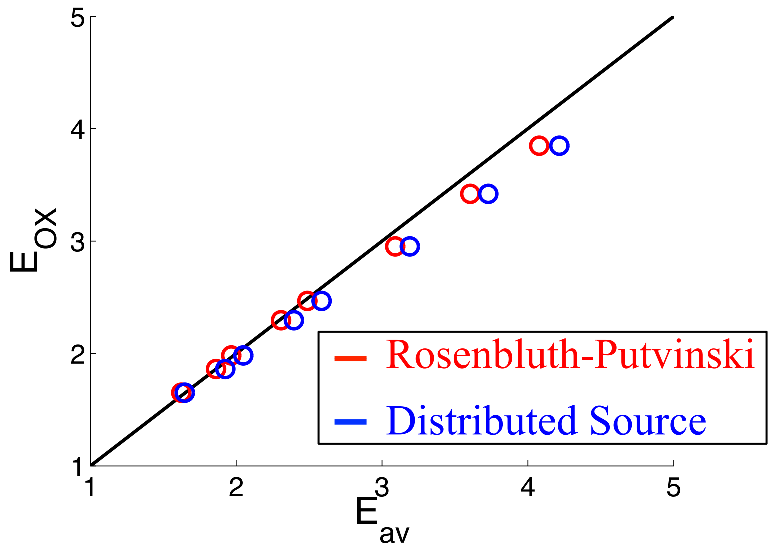

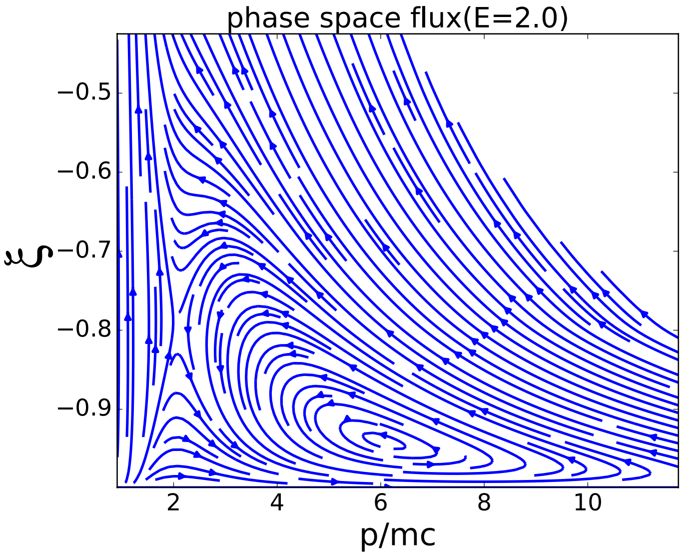

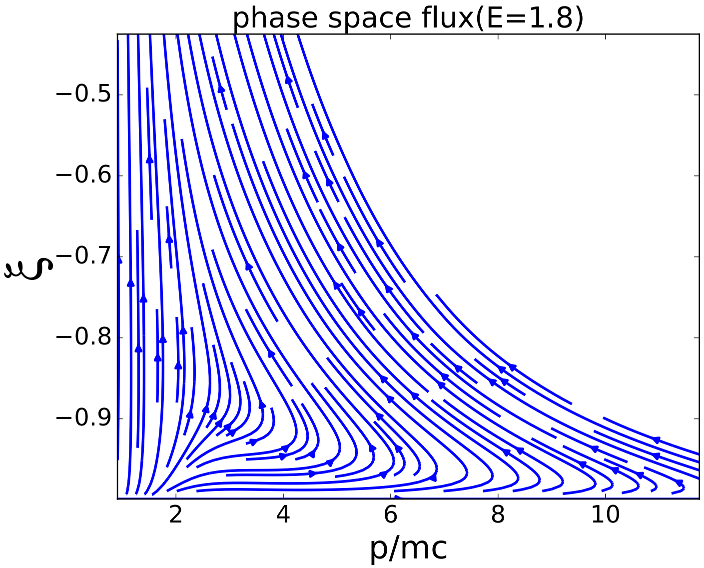

- Runaway vortex ➔ necessary in order to confine runaway electron population at high energy

- Avalanche threshold well correlated with O-X merger over a broad range of parameters:

$$Z = 1 - 10,\ \alpha = \tau_c/\tau_s = 0.05 - 0.3$$

Merger of O-X Points can be Described Analytically

- Location of O and X points set by the crossing of the $\Gamma_p = 0$ and $\Gamma_\xi = 0$ surfaces

$$\Gamma_p = \left[-\xi \bar{E} - C_F - \alpha p \gamma \left(1 - \xi^2\right)\right] f_e = 0$$

$$\Gamma_\xi = -\left(1 - \xi^2\right) \left(E - \alpha \frac{p}{\gamma} \xi + \frac{C_B}{p} \frac{\partial \ln f_e}{\partial \xi} \right) f_e = 0$$

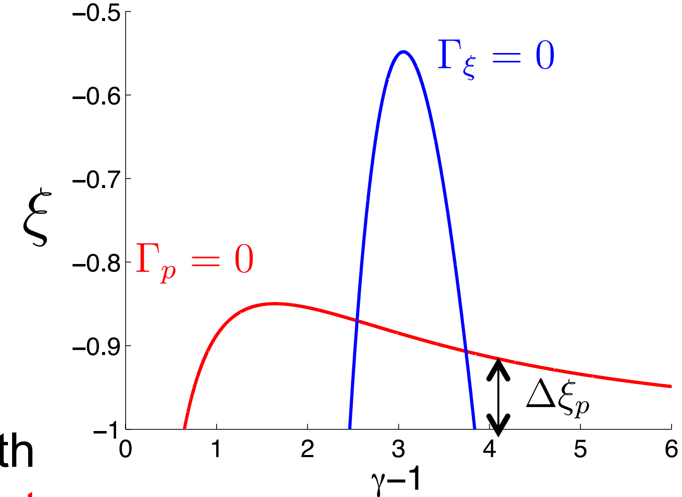

- Width of pitch-angle distribution to scale with the width of the runaway region $\Delta\xi_p$ [Decker et al. 2016, Guo et al., 2017]

$$\Delta\xi = \sqrt{2}\Delta\xi_p \approx \sqrt{2}\frac{\bar{E} - 1 - p^{-2}}{2\alpha p \gamma + \bar{E}}$$

- Allows location of $\Gamma_p = \Gamma_\xi = 0$ surfaces to be estimated:
  - Provides physics based means of estimating O-X merger ⇔ model can be easily extended to include a variety of physical processes

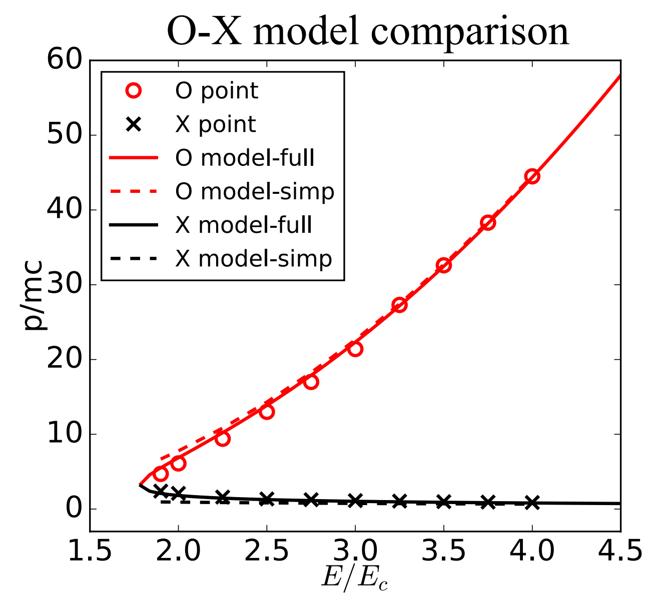

Avalanche Threshold: O-X Merger

- The avalanche threshold is closely tied to the O-X merger
  - Presence of an O-point necessary to sustain a runaway population
  - Avalanche threshold is largely independent of whether Rosenbluth-Putvinski source or more comprehensive source of secondary electrons is used
- Close agreement for a range of values of synchrotron radiation/Z numbers

$$Z = 1 - 10,\ \alpha = \tau_c/\tau_s = 0.025 - 0.3$$

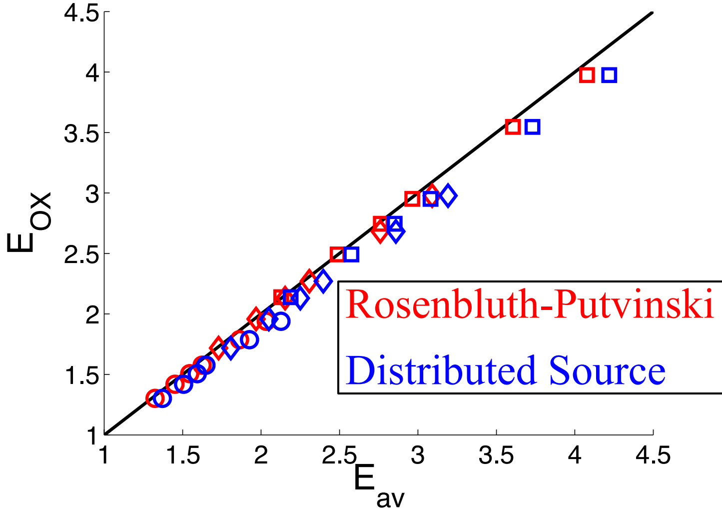

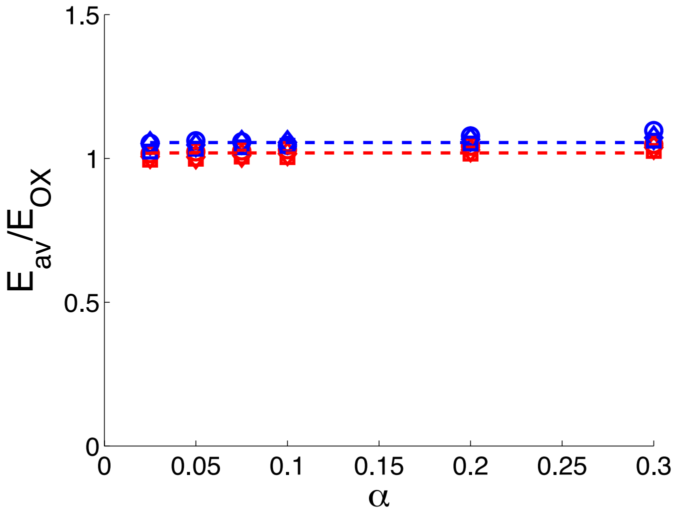

Outline

- Runaway Vortex: Momentum space topology of primary runaway distribution function
- Link of avalanche threshold to momentum space topological change ⇔ O-X merger (disappearance of runaway vortex)
- Self-consistent formulation of small and large angle collisions ➔ Impact on avalanche threshold and growth rate

Energy Dependent Coulomb Logarithm for Runaway Electrons

- The Coulomb logarithm for relativistic electrons can deviate significantly from that of thermal electrons

- Defining $\ln\Lambda = \ln b_{max}/b_{min}$, where $b_{max} = \lambda_D$, $b_{min} = \max\left(b_0, \lambda_{dB}\right)$

- However, both the classical distance of closest approach b_0 and the de Broglie wavelength λ_{dB} scale with the relative momentum between colliding electrons:

$$b_0 \sim \frac{1}{\bar{p}^2}, \quad \lambda_{dB} \sim \frac{1}{\bar{p}}, \quad \ln\Lambda_{rel} > \ln\Lambda_{Te}$$

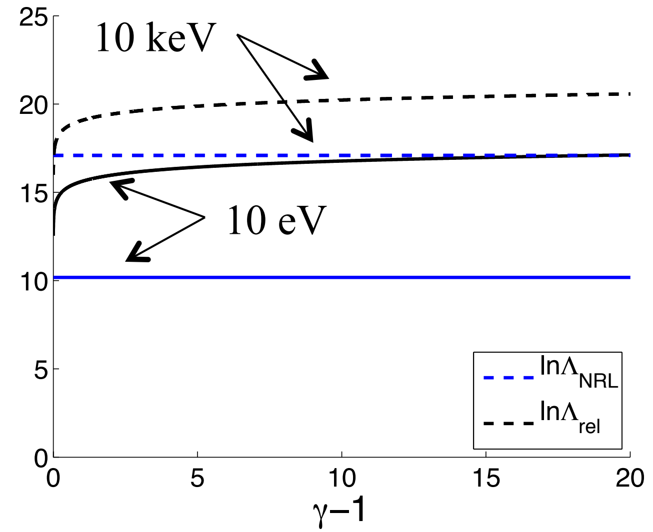

- Thus, $b_{min} \ll b_{min}^{Te}$, $\ln\Lambda_{rel} > \ln\Lambda_{Te}$, for relativistic electrons, $\lambda_{dB}/b_0 \approx 137/2$ hence [Solodov-Betti 2009]:

$$\boxed{\ln\Lambda_{rel}\left(p\right) = \ln\frac{\lambda_D}{\lambda_{dB}\left(p\right)}}$$

  - Form described in [Mosher 1975, Martin-Solis 2017] for free-free collisions use $b_{min} = b_0$ ➔ leads to significantly larger Coulomb logarithm

Conservative Large-Angle Collision Operator

- Large-angle collisions often incorporated via a knock-on “source”
  - Primaries evolved by Fokker-Planck collision operator
  - Leads to inconsistent formulation ⇔ large-angle scattering of primary electrons not accounted for

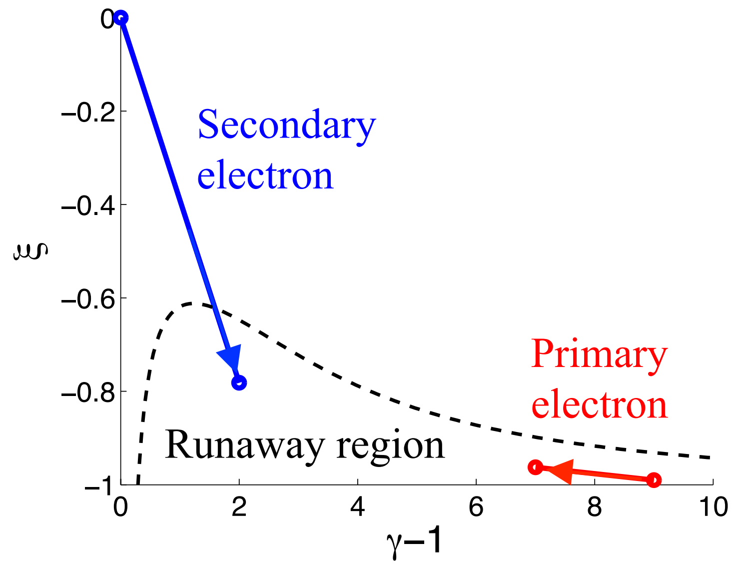

- Redistribution of primaries can be accounted for by considering complete form of linearized Boltzmann collision operator:

$$\boxed{\begin{aligned}\left.\frac{\partial f_e}{\partial t}\right|_{LA} &= \frac{n_b}{2\pi p^2}\int d^3p' v' \frac{d\sigma_M\left(p',p\right)}{dp}\Pi\left(p',\xi',p;\xi\right) f_1\left(\mathbf{p}'\right) \\ &\quad - \frac{1}{2}n_b\delta\left(\mathbf{p}\right)\int d^3p_1 v_1 \sigma_M\left(p_1\right) f_1\left(\mathbf{p}_1\right) - \frac{1}{2}n_b v\sigma_M\left(p\right) f_1\left(\mathbf{p}\right)\end{aligned}}$$

  - Ensures energy and momentum conservation from large-angle collisions

Conservative Large-Angle Collision Operator

- Large-angle collisions often incorporated via a knock-on "source"
  - Primaries evolved by Fokker-Planck collision operator
  - Leads to inconsistent formulation ⇔ large-angle scattering of primary electrons not accounted for

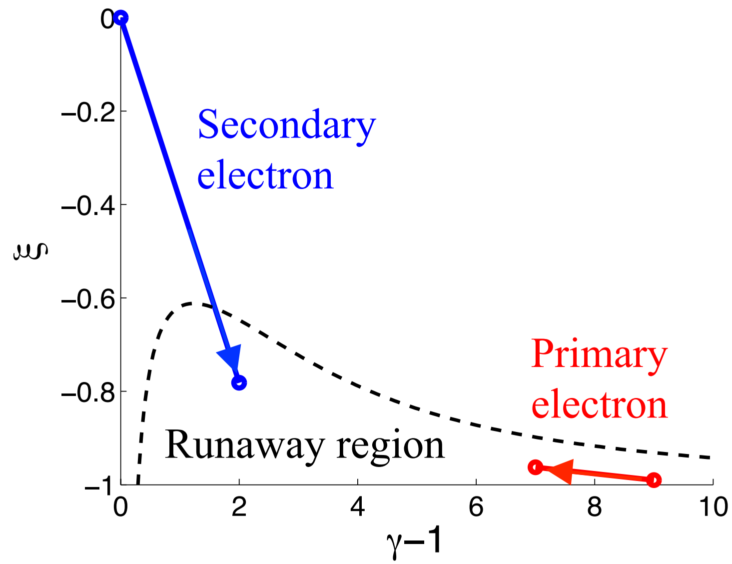

- Redistribution of primaries can be accounted for by considering complete form of linearized Boltzmann collision operator:

$$\left.\frac{\partial f_e}{\partial t}\right|_{LA} = \frac{n_b}{2\pi p^2}\int d^3p' v' \frac{d\sigma_M\left(p',p\right)}{dp}\Pi\left(p',\xi',p;\xi\right) f_1\left(\mathbf{p}'\right) \cancel{-\frac{1}{2}n_b\delta\left(\mathbf{p}\right)\int d^3p_1 v_1\sigma_M\left(p_1\right) f_1\left(\mathbf{p}_1\right)} - \frac{1}{2}n_b v\sigma_M\left(p\right) f_1\left(\mathbf{p}\right)$$

Neglected here

- Ensures energy and momentum conservation from large-angle collisions

Back Reaction onto Primary Electrons

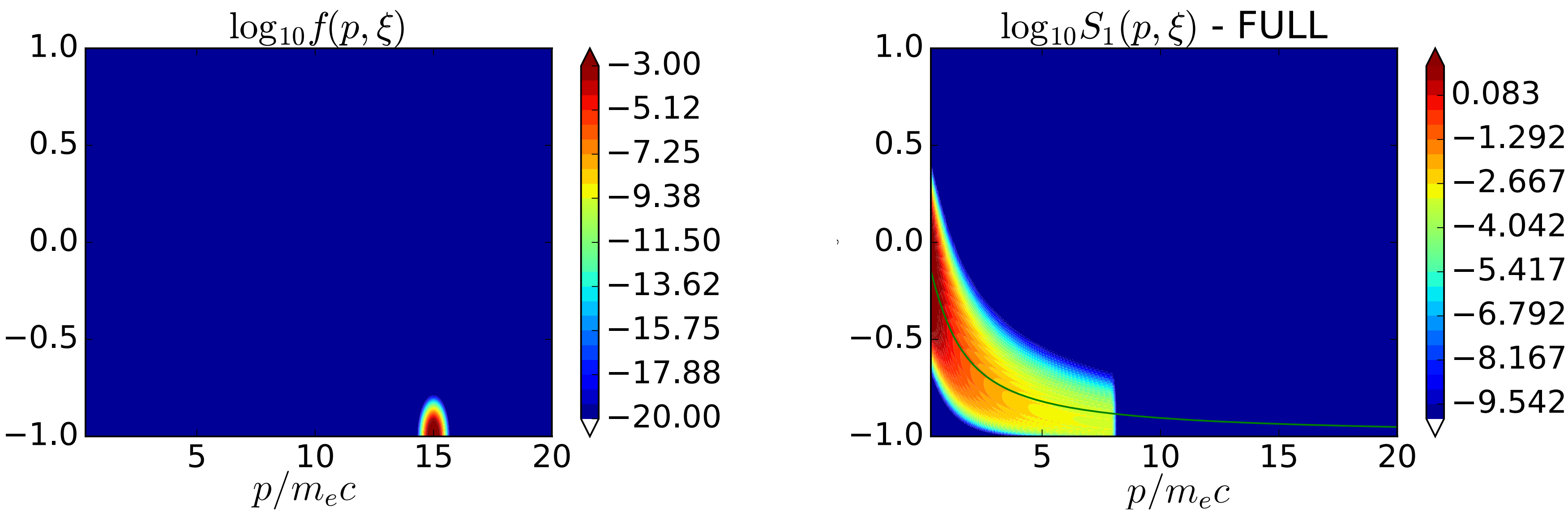

Back Reaction onto Primary Electrons

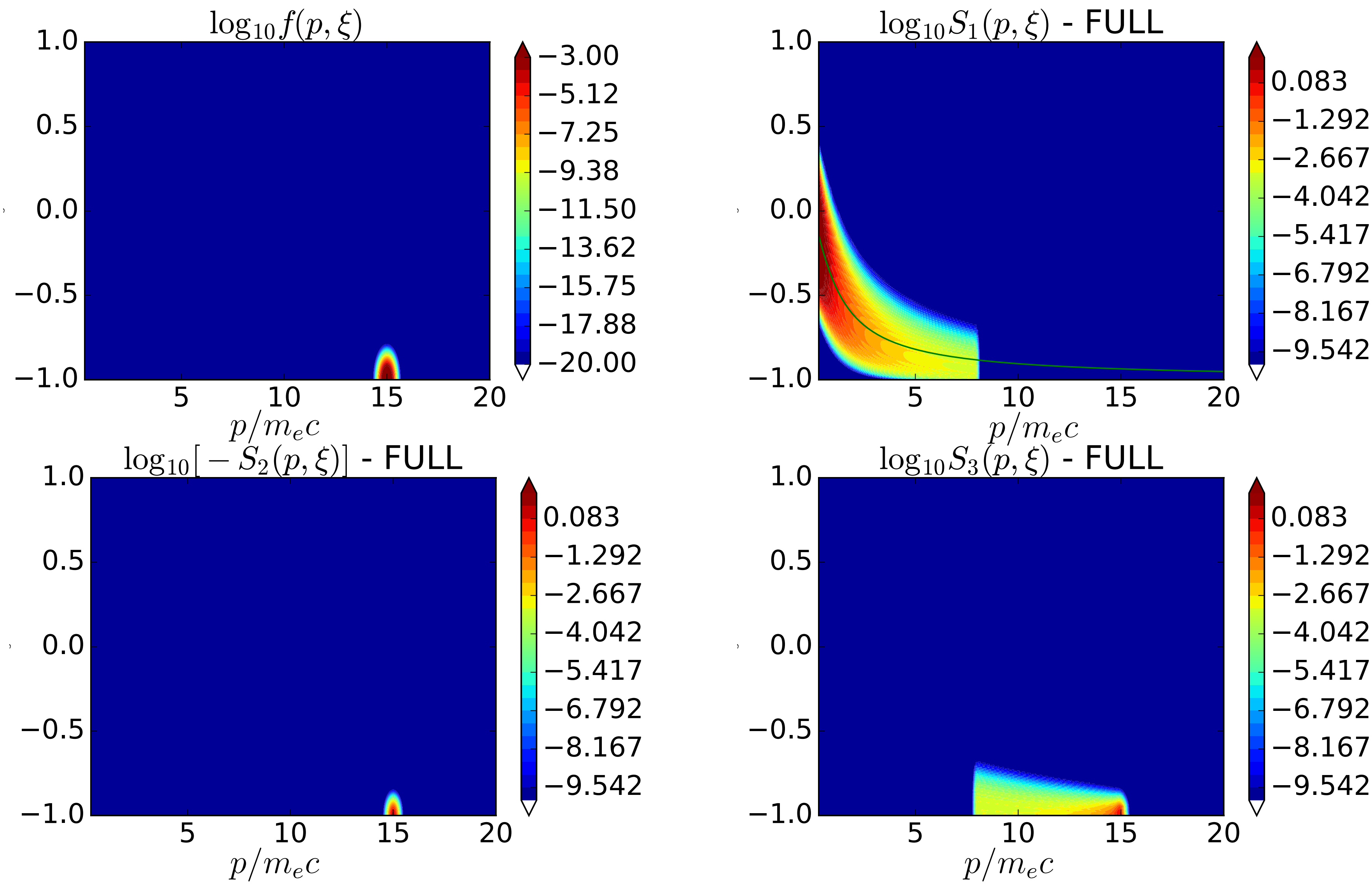

Avoiding Double Counting Collisions

- Addition of down scattering terms can result in double counting collisions

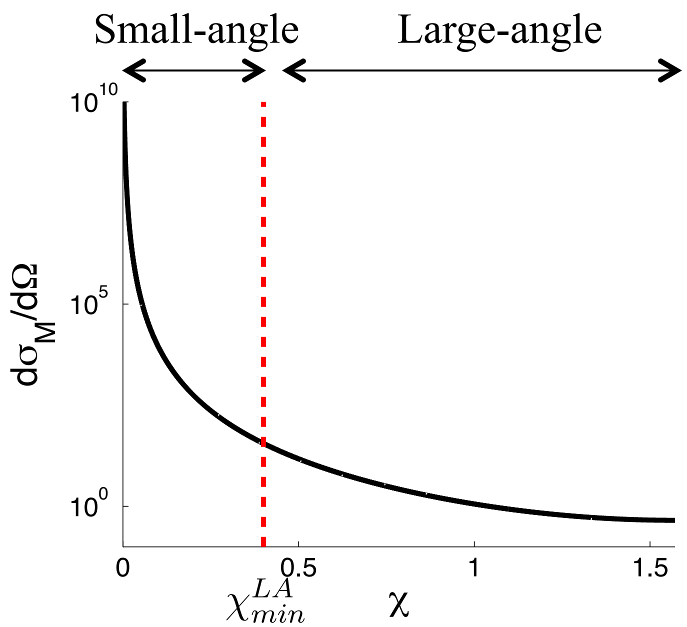

Avoiding Double Counting Collisions

- Addition of down scattering terms can result in double counting collisions

- The choice of an intermediate cutoff angle can be constrained by noting:
  1. The large-angle collision operator assumes the thermal electron population to be cold:

$$\boxed{m_e c^2 \left(\gamma_{min} - 1\right) \gg m_e v_{Te}^2/2}$$

  2. Only secondary electrons whose energy is greater/comparable to the X point location can runaway:

$$\boxed{\gamma_{min} - 1 < \gamma_X - 1}$$

- Center-of-mass scattering angle χ_{min}^{LA} related to γ_{min} by:

$$\sin^2 \frac{\chi_{min}^{LA}}{2} = \frac{\gamma_{min} - 1}{\gamma - 1}$$

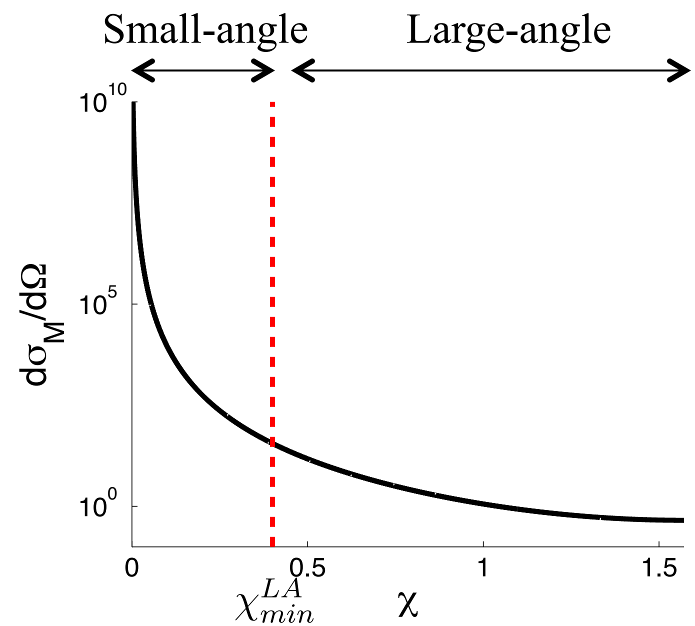

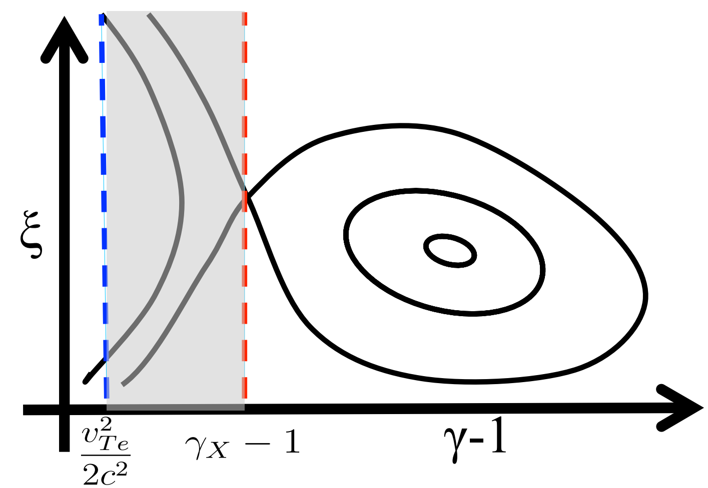

Modified Coulomb Logarithm

- Introduction of additional cutoff angle modifies Coulomb logarithm used in Fokker-Planck equation

- The drag coefficient in the Fokker-Planck equation is proportional to:

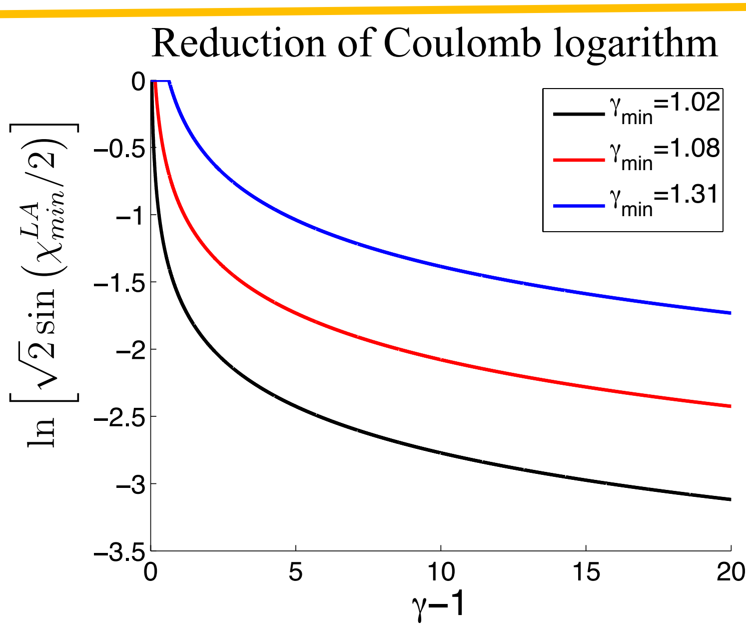

$$\frac{\langle \Delta p \rangle}{\Delta t} \sim \int_{\chi_{min}}^{\chi_{min}^{LA}} d\chi \sin\chi \sin^2\frac{\chi}{2}\frac{d\sigma_m}{d\Omega} \sim \ln\left[\frac{2}{\chi_{min}}\sin\left(\chi_{min}^{LA}/2\right)\right] + \mathcal{O}\left(1\right)$$

- Coulomb logarithm reduced by a factor:

$$\boxed{\ln\left[\sqrt{2}\sin\left(\chi_{min}^{LA}/2\right)\right] \leq 0}$$

  - Leads to a significant reduction of Coulomb logarithm used in Fokker-Planck equation (10-20%)

Sensitivity to Intermediate Cutoff

- Necessary to assess the sensitivity of the avalanche growth rate to the intermediate cutoff angle [$\chi_{min}^{LA} = \chi_{min}^{LA}(\gamma_{min})$]
- Broad regime of insensitivity evident:
  - For γ_{min} too large, the avalanche growth rate underestimated ⇔ incorrectly omits secondary electrons
  - Formalism invalid for energies comparable to the thermal energy

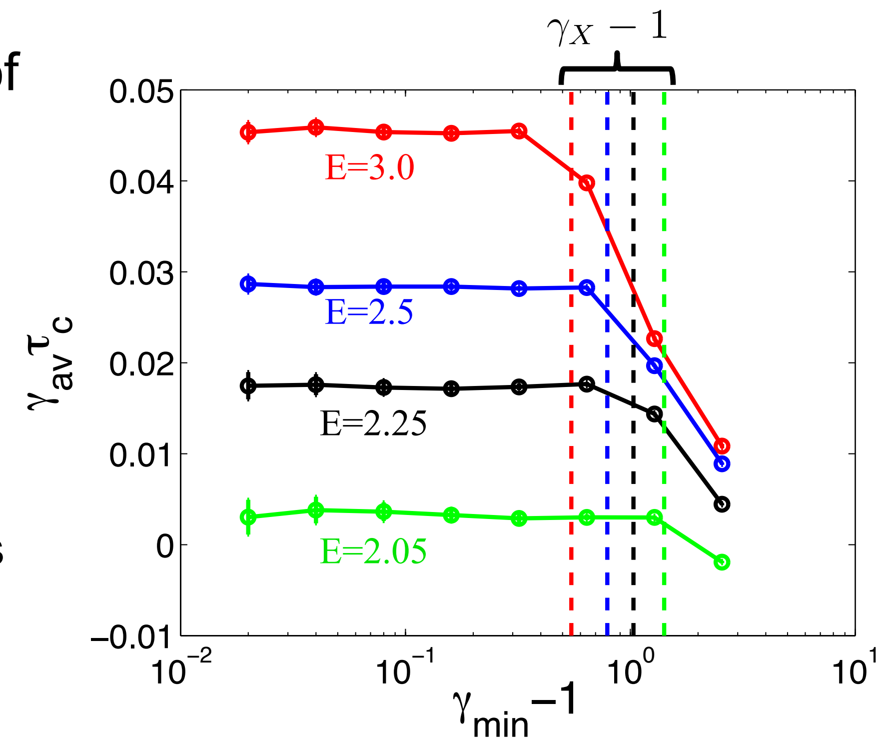

Contrasting Current Model with Previous Model

- Addition of conservative large-angle collision operator + modified Coulomb logarithm reduces avalanche growth rate

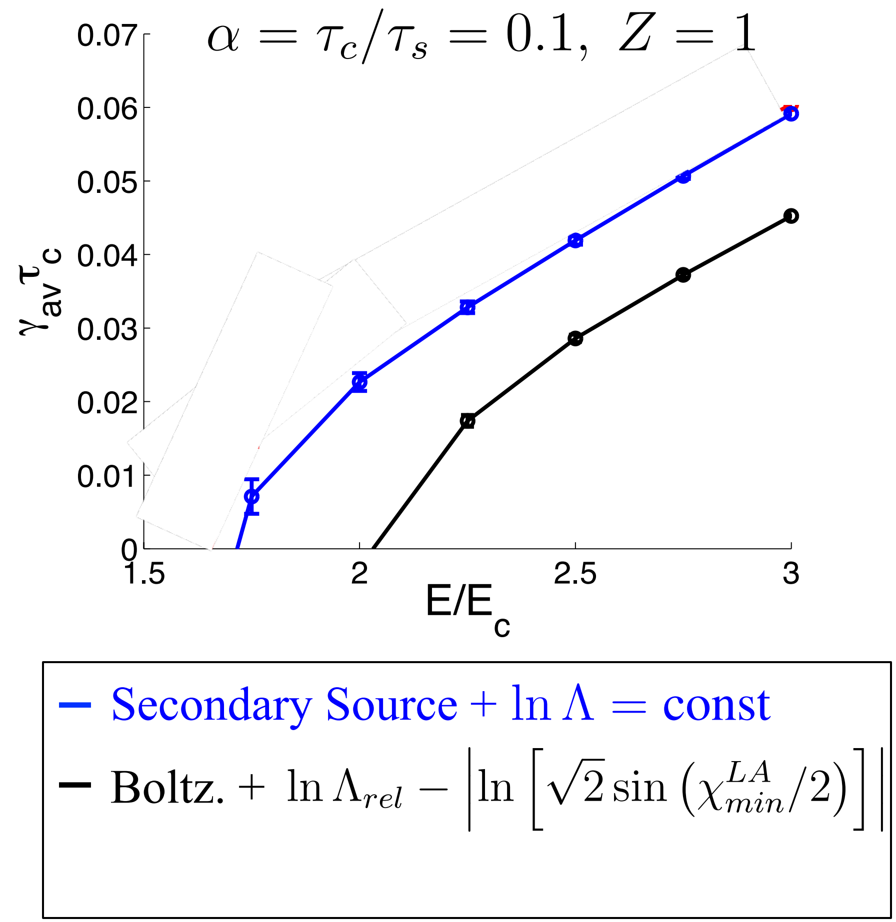

Contrasting Current Model with Previous Model

- Addition of conservative large-angle collision operator + modified Coulomb logarithm reduces avalanche growth rate
- Useful to identify which additional physics has the strongest impact on avalanche growth rate:
  - Consider additional case with $\ln\Lambda = \ln\Lambda_{rel}(p)$, but without conservative large-angle collision operator
  - Conservative large-angle collision operator has a modest impact on avalanche growth rate once double counting constraint is accounted for!

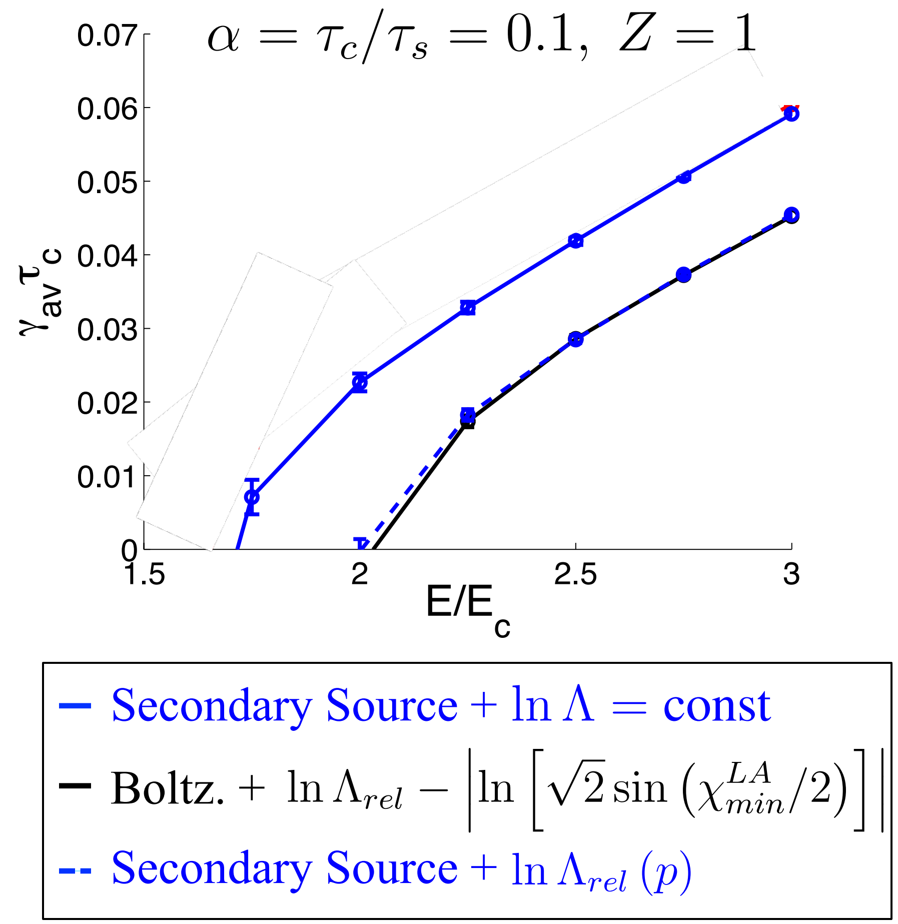

Impact of Large-Angle vs. Small-Angle Collisions

- Use of conservative large-angle collision operator involves a tradeoff:
  1. Introduces additional down-scattering of primary electrons
  2. To avoid double counting, Coulomb logarithm is reduced by:

$$\ln\Lambda = \ln\Lambda_{rel} - \left|\ln\left[\sqrt{2}\sin\left(\frac{\chi_{min}^{LA}}{2}\right)\right]\right|$$

- Both modifications scale with $1/\ln\Lambda$
  - Leads to modest impact on avalanche growth rate

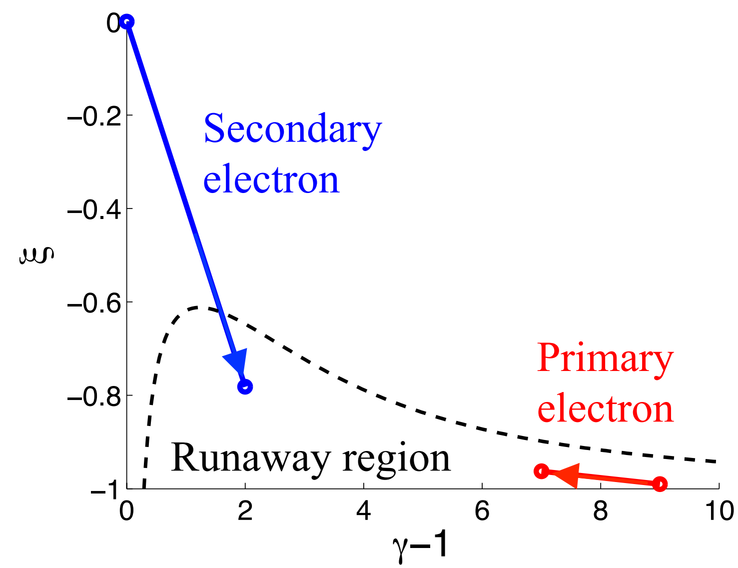

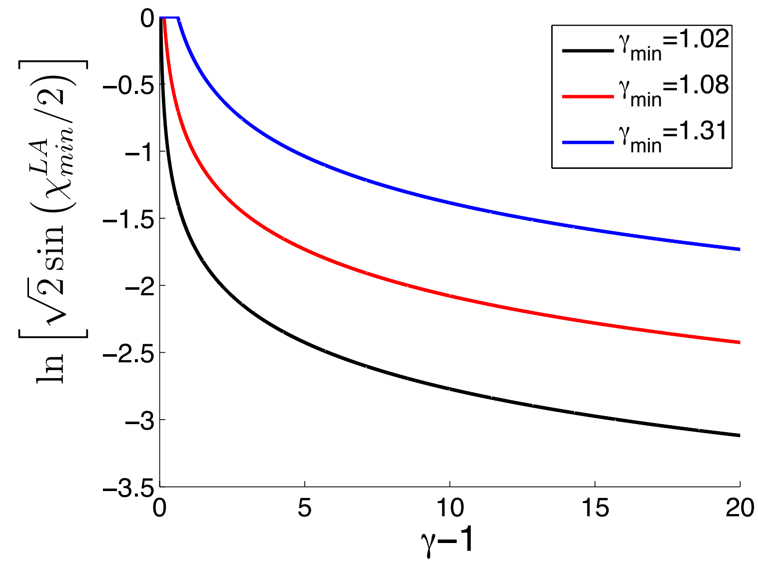

Avalanche Threshold Well Described by O-X Merger

- O-X merger model of primary distribution can be modified to incorporate a more accurate Coulomb logarithm
- Predicted avalanche threshold in good agreement with O-X merger for a broad parameter range

$$Z = 1 - 10,\ \alpha = \tau_c/\tau_s = 0.025 - 0.3,$$
$$\ln \Lambda_{NRL} = 5 - 20$$

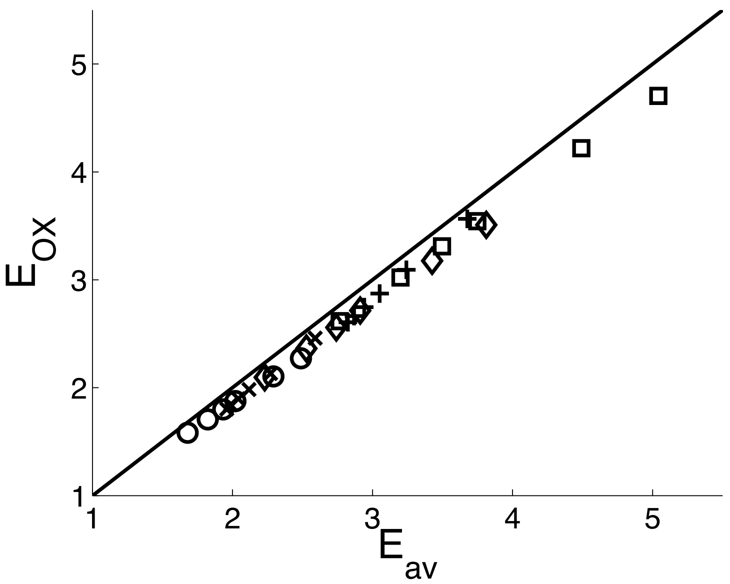

$$\boxed{\text{Boltz.} + \ln \Lambda_{rel} - \left| \ln \left[\sqrt{2} \sin \left(\chi_{min}^{LA}/2 \right) \right] \right|}$$

Conclusions

- O-X merger of primary distribution identified as a reliable indicator of avalanche instability ⇔ runaway vortex necessary to confine runaway electron population:
  - A robust, and highly malleable, analytic model describing the O-X merger of the primary distribution has been developed
- A conservative large-angle collision operator appropriate to the description of runaway electrons has been derived:
  - Systematic procedure for delineating small and large angle collision operators developed
- A more comprehensive avalanche model that self-consistently treats large-angle scattering events and incorporates a Coulomb logarithm appropriate for runaway electrons has been derived
  - Significantly modifies the avalanche growth rate and threshold

Relation of Avalanche Threshold to Features of Primary Distribution

- Interested in identifying how the avalanche threshold is correlated with features of the primary distribution function
- We will consider a comparison with two features of the primary distribution:
  1. Merger of O-X point ⇔ necessary in order to confine runaway electron population at high energy [Guo et al. 2017]
  2. Formation of a pitch-angle averaged bump ⇔ prominent role in attractor picture [Aleynikov-Breizman 2014]
- Avalanche threshold most closely correlated with O-X merger over a broad range of parameters:

$$Z = 1 - 10,\ \alpha = \tau_c/\tau_s = 0.05 - 0.3$$

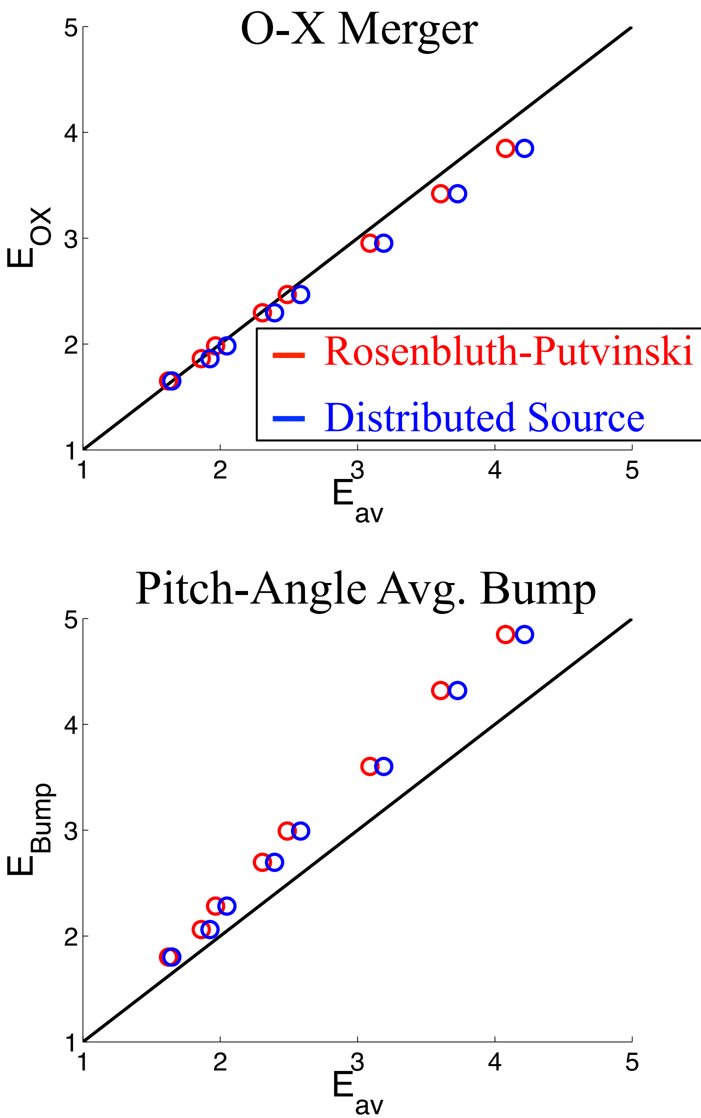

Los Alamos NATIONAL LABORATORY EST. 1943

NNSA